PHYSICAL REVIEW B **75**, 144113 (2007)

Perturbation theory for classical solids with vacancy defects

Sunil P. Singh and Shankar P. Das*
School of Physical Sciences, Jawaharlal Nehru University, New Delhi 110067, India

(Received 7 August 2006; revised manuscript received 15 December 2006; published 26 April 2007)

We present a density functional model for the thermodynamic properties of a Lennard-Jones system in the crystalline state having a small fraction of vacancies present in the lattice. The test density function is modified from its usual form to take into account the presence of vacancies in the lattice structure. The repulsive part of the Lennard-Jones potential is treated in terms of an equivalent hard sphere (EHS) system while the contribution from the long attractive part is treated perturbatively. The properties of the EHS in the inhomogeneous state is obtained with the weighted density functional approach. The thermodynamic behavior is studied by locating the state of minimum free energy. The dependence of the vacancy concentration on temperature at the coexistence of crystal and liquid is obtained.

DOI: 10.1103/PhysRevB.75.144113 PACS number(s): 61.50.Ah, 61.72.Bb, 61.72.Ji

I. INTRODUCTION

The thermodynamic properties of macroscopic systems are obtained from models based on the statistical mechanics of many particle systems. At the microscopic level the system is described in terms of the basic interaction potential between the particles. In the theoretical models one usually deals with the systems that have hard sphere or purely repulsive type interactions. Systems with attractive potentials on the other hand have been studied by formulating a perturbative expression for the thermodynamic properties.[1] This approach involves splitting the interaction potential into a short range purely repulsive and a long range attractive part. The thermodynamic property of the system with the given interaction potential is then obtained as a sum of two contributions: that of a reference system having the purely repulsive interaction and the contribution coming from the attractive part of the interaction treated perturbatively. In the first part, the properties of the reference system are usually known from independent models. The most commonly used reference system is the hard sphere potential for which there exist several models accurately describing the thermodynamic properties of the homogeneous state for densities ranging from low to very high values. The diameter of this equivalent hard sphere system is determined from suitable criteria[2] obtained from thermodynamic considerations. However such theories for more generalized potentials are dealing with the uniform liquid state rather than the nonuniform solid state.

The theoretical models of classical solids having strongly inhomogeneous density distributions is also formulated in terms of the basic interaction potential. In this regard the density functional theory (DFT)[3–5] has been a very useful tool for studying the thermodynamic properties of the nonuniform state. It provides a suitable methodology for computing the thermodynamic properties of the solid state in terms of those of the liquid state. Here also the theoretical studies have been initially focused on the systems with hard sphere interactions. For systems with interaction potentials having an attractive part, the free energy is computed (in a mean-field approach) by adding a correction to the free energy of a system having a purely repulsive interaction. The correction term is obtained in a perturbative approach in which[6] the structural properties of the reference solid state is substituted in terms of that of an uniform liquid. However, Recently Rascón *et al.* have improved the calculation of the free energy of the solid whose interaction potential has an attractive part. This involves obtaining an approximate solid state structure factor of the reference system which is then used in the perturbative expression for the free energy. In the present work we follow this approach to study the inhomogeneous solid state of a one component Lennard-Jones (LJ) system having *vacancy defects*. The reference system here is described in terms of a similar imperfect hard sphere system with vacancy. The structure factor for the latter is obtained using in the standard density functional model a modified density function. This inhomogeneous density takes into account the absence of particles in a small fraction of the lattice sites. Since the density of vacancies in the crystal is so small we ignore the interaction between the defects in the solid. The interaction part of the free energy for the solid is obtained using the modified weighted density functional approximation (MWDA), which is a more effective way of computing the thermodynamic properties of the strongly inhomogeneous crystalline state. The structure factor of the solid state is computed approximately following Ref. 7. The paper is organized as follows: In Sec. II we describe the modification of the density function in terms of which the DFT is formulated. Here we also describe the choice of the proper reference system and computation of the solid state structure factor. In Sec. III the computation of the free energy for the LJ system is outlined and the optimum value of the defect concentration in the equilibrium state is obtained. In Sec. IV we discuss our results and other related works on LJ solids with defects.

II. DESCRIPTION OF THE MODEL

We consider the crystal being represented statistically by a canonical ensemble having N number of particles in volume V at temperature T. The basic interaction potential between the particles is used as a starting point in the model. In the present work we consider the system interacting through the Lennard-Jones potential which has a hard core repulsive part and a long range attractive part. The free energy of the

1098-0121/2007/75(14)/144113(9)

solid is expressed as a function of inhomogeneous density function $n(\mathbf{r})$. The theory uses a suitable parametric description for the nonuniform density function and is defined as a sum of Gaussian profiles[8] centered at each lattice site of the crystalline structure,

$$n(\mathbf{r}) = \sum_{\mu=1}^{N} \phi_\alpha(|\mathbf{r} - \mathbf{R}_\mu|), \quad (1)$$

where $\phi_\alpha(\mathbf{r})=(\alpha/\pi)^{3/2}e^{-\alpha r^2}$ is the Gaussian function and $\mathbf{R}_\mu$ denotes the position of the μth lattice sites in the solid. The total number of lattice sites in the crystal is N_{PC} of which N sites are occupied by the particles and N_D are vacant ($N_{PC}=N+N_D$). It is assumed here that $N_D \ll N$ and that the vacant sites are not close to each other. The Gaussian density profile is absent for the vacant site. The quantity α in Eq. (1) represents the inverse square width of the Gaussian profiles and will be called the width parameter (WP). The limit $\alpha \to 0$ corresponds to the liquid phase, while high values of α correspond to the inhomogeneous crystal state.

We follow here broadly the perturbative scheme developed earlier[9] for studying the thermodynamic properties for the perfect crystal. The Lennard-Jones potential is divided into two parts,[1] namely a hard core repulsive part (called the reference part) V_{hc} and an attractive potential V_a. The Helmholtz free energy of the fcc solid is then obtained as $F[n(\mathbf{r})]=F_{\text{re}}[n(\mathbf{r})]+F_{\text{mf}}[n(\mathbf{r})]$ where F_{re} and F_{mf}, respectively, denote the reference state free energy and a contribution from the attractive part of the potential. F_{mf} is computed using the mean-field approximation as

$$F_{\text{mf}}[n(r)] = \frac{1}{2}\int\int dr_1 dr_2 f_2(\mathbf{r}_1,\mathbf{r}_2)V_a(r_{12}), \quad (2)$$

where $f_2(r_1,r_2)$ is the two-point distribution function (TPDF) for the crystalline solid state. It represents the probability of simultaneous occurrence of particles 1 and 2, respectively, at $\mathbf{r}_1$ and $\mathbf{r}_2$, irrespective of their momentums. The result (2) can be further simplified as

$$F_{\text{mf}}[n(\mathbf{r})] = 2\pi V \int dr r^2 \tilde{f}_2(r)V_a(r), \quad (3)$$

in terms of the angular averaged TPDF $\tilde{f}_2(r)$ defined as

$$\tilde{f}_2(r) = \int \frac{d\Omega}{4\pi}\int \frac{d\mathbf{r}_1}{V} f_2(\mathbf{r}_1,\mathbf{r}_1+\mathbf{r}), \quad (4)$$

where $d\Omega$ is the differential solid angle aperture around $\mathbf{r}$. Earlier works[6] have used the approximation $\tilde{f}_2(r)=n_0^2 g(r)$, in terms of the uniform liquid state radial distribution function $g(r)$.[10] For a better estimation of the contribution to the free energy from the attractive part of the potential we use following Rascón *et al.*,[9] the solid state $\tilde{f}_2(r)$ for the reference hard sphere system. We next discuss the proper choice for the reference part of the Lennard-Jones potential in the present context.

A. The reference system

The free energy of the purely repulsive reference system is approximated by an expansion in terms of an equivalent hard sphere (EHS) system. Using a statistical mechanical approach[1,11] the reference state free energy is obtained as a perturbative expansion,

$$F_{\text{re}}[n(\mathbf{r})] = F_{\text{HS}}[n(\mathbf{r})] + 2\pi n_0 N \int dr r^2 \tilde{y}_{\text{HS}}(r)\Delta e(r) + O[(\Delta e)^2], \quad (5)$$

where $\tilde{y}_{\text{HS}}(r)$ is the angular average of the hard sphere function $y_{\text{HS}}(\mathbf{r}_1,\mathbf{r}_2)$ and can be expressed as

$$\tilde{y}_{\text{HS}}(r) = e^{\beta V_{\text{HS}}(r)}\tilde{f}_2(r). \quad (6)$$

In terms of the two-point distribution function $\tilde{f}_2(r)$ of the solid state defined above in Eq. (4). V_{HS} is the interaction potential of EHS of diameter σ_E. The latter σ_E is a free parameter in the theory and its value is fixed such that first order term in the expansion of Eq. (5) for the free energy becomes zero. Thus

$$\int_{\sigma_E}^{\infty} dr r^2 \tilde{y}_{\text{HS}}(r) - \int_0^{\infty} dr r^2 \tilde{y}_{\text{HS}}(r)e^{\beta V_{\text{hc}}} = 0. \quad (7)$$

The EHS radius σ_E is therefore computed with the knowledge of the angular averaged TPDF $\tilde{f}_2(r)$. The angular averaged function $\tilde{f}_2$ is also necessary in computing the mean-field term F_{mf} in (3). The computation of $\tilde{f}_2$ defined in (4) of the EHS is therefore the next step in the calculation. In the present context we need to obtain the two-point functions for the imperfect crystal with vacancies. Since the individual particles in a crystal are sharply localized to the site, the TPDF $f_2(\mathbf{r}_1,\mathbf{r}_2)$ is approximated at the simplest level as the product of the individual probabilities, i.e., the single particle densities,

$$f_2(\mathbf{r}_1,\mathbf{r}_2) = n(\mathbf{r}_1)n(\mathbf{r}_2). \quad (8)$$

The approximation for f_2 as a product of single particle densities amounts to neglecting the two-point correlation in the crystal and hence works better when r is large. The inhomogeneous density $n(\mathbf{r})$ for the hard sphere system is expressed as a sum of Gaussian profiles as in (1). We include the presence of vacancies in the lattice through a modification of the density function. The fraction of sites occupied is $N/N_{PC}=\mathcal{A}$. Hence the probability that a given site is occupied by the particles is $\mathcal{A}=N/N_{PC}$, or equivalently $\Delta_v=1-\mathcal{A}$ is the probability that a site is vacant. Computation of f_2 using the definition (8) require the density function $n(\mathbf{r})$. For the imperfect crystal $n(\mathbf{r})$ is now modified with the averaged form,[12] $\tilde{n}(\mathbf{r})=\mathcal{A}n_{pc}(\mathbf{r})$ where the $n_{pc}(\mathbf{r})$ would be the density for the perfect lattice (i.e., for $N=N_{PC}$) in absence of vacancies. Thus the influence of the vacancy is only included in an average manner here in the computation of $\tilde{f}_2$. Using this averaged one particle density function (now parametrized in terms of the WP α_H and $\mathcal{A}$) in the expression (8) the TPDF is calculated. The corresponding angular averaged quantity defined in (4) is obtained in terms of an approximate expression,

$$\tilde{f}^0_2(r) = \sum_i f^0_{2i}(r), \tag{9}$$

where we have used the superscript 0 to denote the approximations mentioned above. The functions $\tilde{f}^0_{2i}(r)$ represent Gaussian peaks which are obtained as

$$f^0_{2i}(r) = \frac{n_0}{4\pi}\sqrt{\frac{\alpha_H}{2\pi}}\left(\frac{w_i}{rR_i}\right)\exp\left(-\frac{\alpha_H}{2}(r-R_i)^2\right), \quad i = 2,3, \ldots , \tag{10}$$

where $\mathbf{R_i}$ is the radius of the ith shell around a lattice site chosen as origin and w_i is the number of sites in the ith shell in the fcc lattice. In reaching the above expressions (10) we have neglected contributions involving exponential terms like $e^{-\alpha(r+R_i)^2/2}$, since in the present case for large α values (corresponding to the highly localized structures in the crystal) such factors are negligible at finite r values.

The approximate expressions (9) and (10) are good enough for large r. For the *first peak* in $\tilde{f}_2(r)$ (corresponding to the shortest r value) however the above mean-field approximation in terms of $f^0_{21}(r)$ is inadequate to account for the small range correlation in the system and requires improvement. The first peak of $\tilde{f}_2(r)$ is therefore obtained using thermodynamic properties of the hard sphere solid. We make the following choice from Ref. 7:

$$\tilde{f}_{21}(r) = \begin{cases} (A_0/r)\exp\left(-\dfrac{\alpha_0}{2}(r-r_0)^2\right) & \text{if } r \geqslant \sigma_c, \\ 0 & \text{otherwise,} \end{cases} \tag{11}$$

where the superscript 0 in $\tilde{f}_{21}$ on the left-hand side (LHS) of (11) is dropped to indicate the different parametrization involved here [from that for $\tilde{f}^0_{2i}$ in (10) discussed above]. The parameters A_0, α_0, and r_0 are determined by numerically solving three coupled nonlinear equations obtained using the following three constraints. First the normalization of the angular average two-point distribution function $\int dr\tilde{f}_2(r)$ done in the first shell is equal to the coordination number in the corresponding crystal structure. Second, the virial equation relating the pressure of the system to the $\tilde{f}_2(\sigma_c)$ at contact. Finally, approximating the $\langle r\rangle$ calculated with the $\tilde{f}_{(21)}(r)$ and with $\tilde{f}^0_{21}$ to be the same. In the scheme for obtaining $\tilde{f}_2(r)$, outlined above, the pressure P and α_H are required at fixed density n_0 and vacancy concentration n_D. To obtain the pressure P, the free energy of the solid is computed using the standard density functional methods for hard core systems. The DFT calculation in this case requires choosing for the hard sphere system a suitable inhomogeneous density function $n(r)$ in terms of the Gaussian profiles of WP α_H. The free energy of this hard sphere system is calculated with the standard modified weighted density functional approximation.[13] The key aspect of this calculation scheme in the present context is the inclusion of vacancies on the lattice structure. This is done here through a modification of the test density function [as described with Eq. (1)] to be used in the DFT. The details of the MWDA are given in the Appendix. The optimum value of α_H is determined from that corresponding to the minimum $F_{\rm HS}$. As outlined above, for computing the constants in the expression (11) for the function $\tilde{f}_2(r)$ at small r the value of the corresponding pressure P is required. The latter is determined here with the numerical derivative with respect to density n_0 of the free energy $F_{\rm HS}$ at the minimum (at a fixed n_D and n_0). Using the optimum α_H and the corresponding value of the pressure P, we obtain the required functions, respectively, given by (10) and (11) needed to compute the angular averaged TPDF,

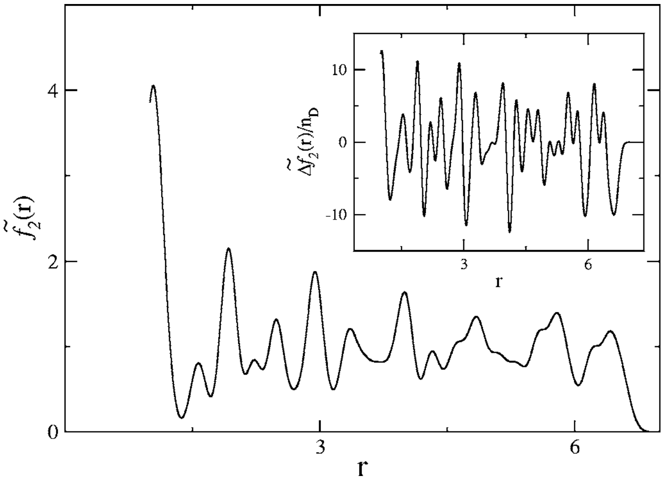

FIG. 1. Angular averaged correlation function $\tilde{f}_2(r)$ for the imperfect hard sphere fcc solid at the density $n_0\sigma^3 = 1.025$. The inset shows the difference of the correlation function $[\tilde{f}^{pe}_2(r) - \tilde{f}^{im}_2(r)]/n_D$ with and without defect at the same density.

$$\tilde{f}_2(r) = \tilde{f}_{21}(r) + \sum_{i=2} \tilde{f}^0_{2i}(r). \tag{12}$$

In Fig. 1 the angular averaged correlation function $\tilde{f}_2(r)$ of the hard sphere fcc solid at density $n_0 = 1.025$ and vacancy density $n_D = 10^{-6}$ is shown. The inset in Fig. 1 displays the difference of the $\tilde{f}_2(r)$ of the perfect crystal and the same for $n_D = 1 \times 10^{-6}$. The effect of the vacancy concentration on the TPDF is also of the order of n_D. It is important to note in this respect that the free energy $F_{\rm HS}$ for the hard sphere system considered above (having WP $\alpha_{\rm HS}$) is different from the free energy $F_{\rm re}$ of the reference system which is a part of the total free energy of the LJ system. Minimization of $F_{\rm HS}$ is only obtained to compute the pair correlation function $\tilde{f}_2(r)$ for the solid state which is then used in Eq. (7) to calculate the diameter σ_E of the EHS system. The reference system is approximated to be another hard sphere system of diameter σ_E, i.e., packing fraction $\eta_0 = \pi n_0 \sigma_E^3/6$. Finally, $\tilde{f}_2(r)$ for the reference system needed for computing the mean-field term in (3), is obtained by rescaling r in terms of σ_E. This completes our description on computing the properties of the reference system.

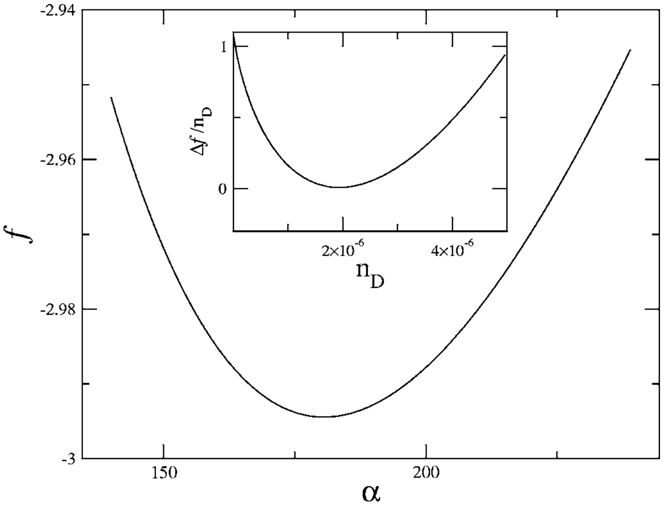

FIG. 2. Free energy βf vs width parameter $\alpha\sigma^2$ corresponding to the optimum defect concentration $n_D\sigma^3=1.9\times10^{-6}$ at $T=1.0$ (in units of ϵ/k_B) and $n_0\sigma^3=1.025$. The inset shows the free energy with respect to $n_D\sigma^3$ corresponding to the optimum value of the width parameter $\alpha\sigma^3=135.41$, at the same temperature and density.

B. The Lennard-Jones system

For a given density n_0 and temperature T of the LJ system we compute the total free energy for the imperfect crystal with vacancy concentration n_D. The stable thermodynamic state is then determined by minimizing the free energy with respect to n_D and the parameters characterizing the density function $n(\mathbf{r})$. The total free energy of the Lennard-Jones system is obtained as a sum of the free energy of a reference system and a mean-field contribution. The free energy of the reference system is now obtained in terms of that of the EHS system of packing fraction η_E and the two-point function $\tilde{f}_2(r)$. The free energy of the EHS system F_{re} is obtained following again the MWDA procedure outlined in the Appendix. The corresponding density function (1) for the EHS system is now expressed in terms of the Gaussian WP α. Thus F_{re} is determined at the corresponding chosen values of n_D and α. The mean-field term F_{mf} in (3) is computed with the characteristic $\tilde{f}_2(r)$ for the EHS system. The sum of F_{re} and F_{mf} is the free energy of the Lennard-Jones system at the chosen value of the WP α and n_D. We now minimize the total free energy with respect to these two parameters to identify the stable equilibrium state of the Lennard-Jones solid at a given n_0 and T. The optimum value of n_D thus obtained is the equilibrium concentration of vacancies in the corresponding thermodynamic state. In Fig. 2 we have shown the minimum of the free energy with respect to the variation of the WP α, while the vacancy concentration n_D is kept fixed at the optimum value. The inset shows the minimum of the free energy in the n_D space at the optimum value of the width parameter α.

The Helmholtz free energy of the imperfect crystal is found to be less than that for the perfect crystal, showing that the presence of vacancies make the crystal thermodynamically more stable than the perfect crystal. In Fig. 3 we compare the free energy of the crystal obtained theoretically form this calculation within the present DFT approach and the computer simulation results for the free energy of the LJ solid.[14] The improvement of the free energy calculation with two-point correlation function[7] for the inhomogeneous state results in very good agreement of theory and simulation data. The free energy of the uniform Lennard-Jones liquid obtained from computer simulations[15] is also shown in the same figure to compare the relative stability of the two phases. Crossover of the free energy occurs at the $T_m=1.10$ below which the crystal state is more stable than the liquid state.

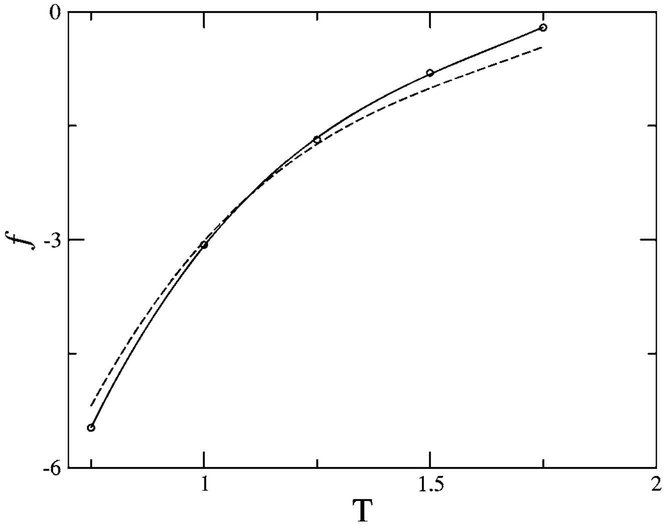

FIG. 3. Free energy βf of the crystal from present theory (solid line), from simulation (open circle). Also shown is the liquid state free energy (dashed line) from computer simulations.

III. NUMERICAL RESULTS

Using the scheme of the DFT outlined above, the optimum vacancy density n_D is computed for a given thermodynamic state of the LJ system of density n_0 and temperature T. We study the variation of n_D with either one of T or n_0, respectively, keeping the other thermodynamic parameter constant. The optimum defect concentration near the freezing is obtained as 6×10^{-6}. Figure 4 shows the variation of n_D with temperature T, at constant density $n_0=1.0$. The inset is described in the context of an improvement in the present model later in the discussion section. The defect concentration decreases exponentially with decrease of the temperature in the manner $n_D/n_0\sim\exp(-\beta\epsilon_v)$. The corresponding activation energy ϵ_v is obtained from the slope of the curve. If on the other hand, the temperature is kept constant, n_D decrease with the increase of density n_0. This dependence at constant $T=1.0$ is shown in the Fig. 5. The decreases of n_D with density here is even more drastic than exponential. We have also studied the temperature dependence of the optimum value of n_D (corresponding to the free energy minimum) along the constant pressure line. The pressure of the fcc solid in this case is computed from the derivative $P=-(\partial f/\partial n_0)_T$, at fixed temperature. This also allows us to study the equation of state for the LJ solid. The variation of

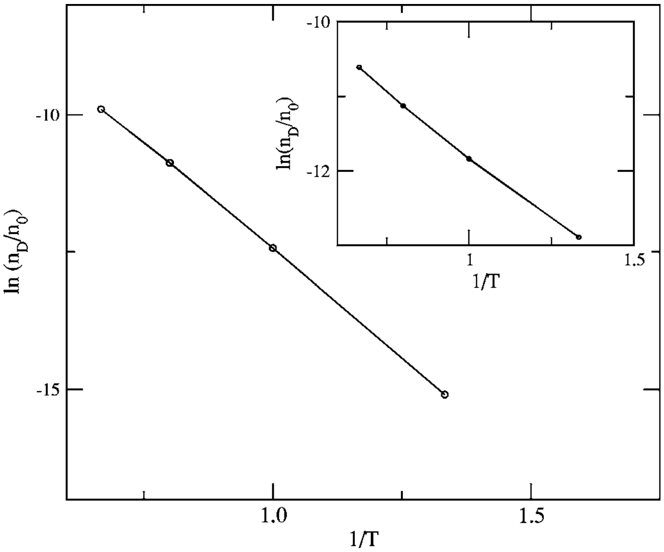

FIG. 4. Relative defect density $\ln(n_D/n_0)$ vs the inverse of temperature T^{-1} (in units of k_B/ϵ) at fixed density $n_0\sigma^3=1.0$. In the inset we display the same quantities obtained in an improved model with two different types of density profiles, respectively, for the normal and the distorted sites (see the discussion section).

pressure P with density n_0 at constant temperature $T=1.0$ is shown in Fig. 6. The pressure P for the liquid state, as obtained from computer simulations[15] is also shown here for comparison. In Fig. 7 the logarithm of the relative defect concentration $\ln(n_D/n_0)$ vs inverse temperature T^{-1} is displayed at fixed pressure $P=3.50$. The defect density decreases on lowering the temperature at constant pressure, the linearity of the curve implying that n_D decreases exponentially with the fall of temperature. We have also calculated defect density dependence on the change of pressure. This is shown in Fig. 8 which displays n_D obtained by changing the pressure at a constant temperature $T=1.0$. The defect density is decreases exponentially with pressure P.

Next, we study the properties of the LJ system in a situation when the crystalline and the liquid state coexist. We consider the variation of the vacancy concentration with temperature of the LJ solid along the coexistence line. For this we require information of the liquid state free energy as well as the corresponding equation of the state. Here we use the computer simulation results of the pressure and free energy as reported by Nicolas *et al.*[15] We have calculated the chemical potentials (μ) of the solid and liquid states from the relation, $\mu=f-Pv$ where f is Helmohtz free energy per particle and $v=1/n_0$ is the specific volume. For the pressure and the free energy of the liquid state we use the computer simulation results. At coexistence the chemical potentials μ and the pressures P for the solid and liquid states are simultaneously equal. At a given temperature there exist only one pair of densities, respectively, corresponding to the coexisting liquid and solid states. In Fig. 9 these coexisting densities

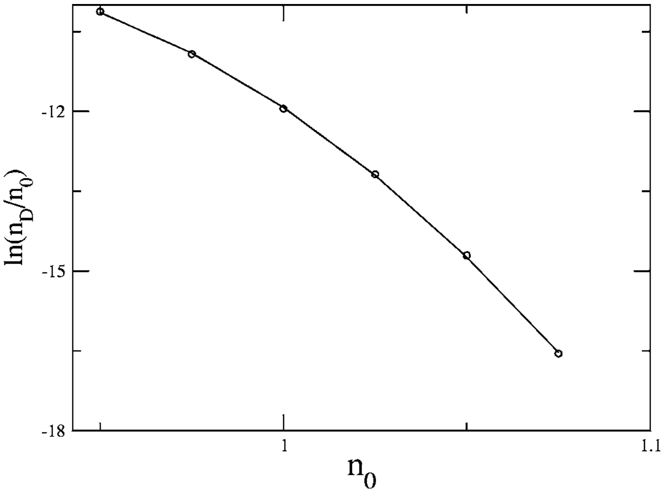

FIG. 5. Relative defect concentration $\ln(n_D/n_0)$ vs the density $n_0\sigma^3$ at fixed temperature $T=1.0$ (in units of ϵ/k_B).

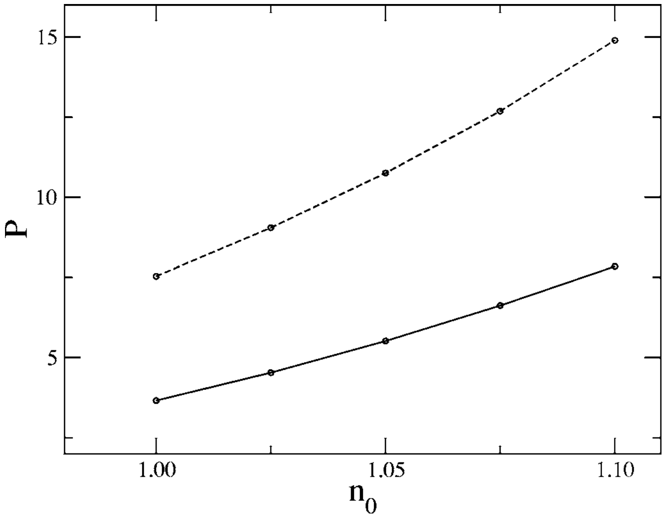

FIG. 6. Pressure P (in units of $\beta\sigma^3$) of uniform liquid (dashed line) and of the crystal (solid line) vs density $n_0\sigma^3$ at temperature $T=1.0$ (in units of ϵ/k_B).

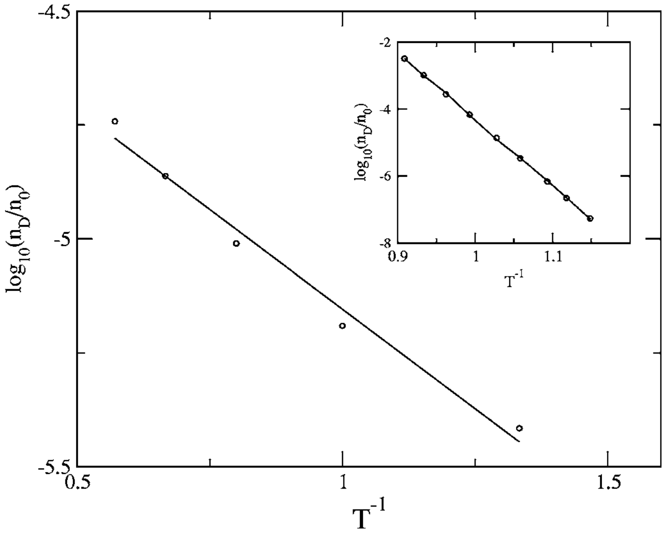

FIG. 7. Relative defect density $\ln(n_D/n_0)$ vs inverse temperature T^{-1} (in units of k_B/ϵ) at fixed pressure $P=3.50$ (in units of $\beta\sigma^3$). The inset shows results from Ref. 18 at pressure $P=2.20$ (pressure is in units of $\beta\sigma^3$).

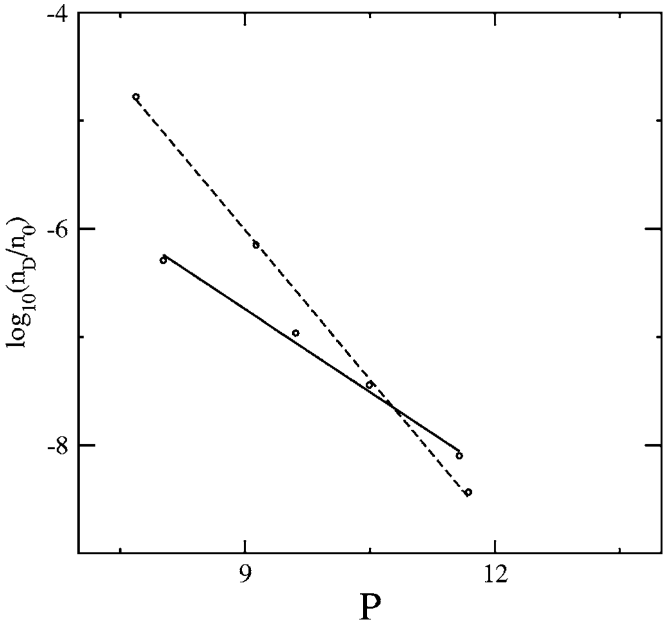

FIG. 8. Relative defect density $\ln(n_D/n_0)$ with respect to pressure P in units of $\beta\sigma^3$ at temperature $T=1.5$ in units of ϵ/k_B (solid line). Results from Ref. 19 at the same temperature are also shown as the dashed line.

(respectively, of the solid and liquid states) vs the corresponding temperature is displayed. Note that here the displayed pairs of coexisting densities, each correspond to a common value for the pressure and the chemical potential. At high temperatures the coexisting densities are also high. The calculation in this limit is not very accurate due to the poor approximation of using the Percus-Yevick direct correlation function at high density. The variation of n_D along the coexistence line shown in Fig. 10 display its decreases with the increase of the temperature. This trend of decreasing vacancy density n_D with increasing temperature is in fact opposite to what was stated above for the crystal state along a constant density or constant pressure line. In the former case, i.e., along the coexistence line, as the temperature increases the density *also increases* instead of decreasing (which would have been the case for change of temperature along the constant pressure line). The observed n_D behavior is mainly controlled here by the increasing crystal density.

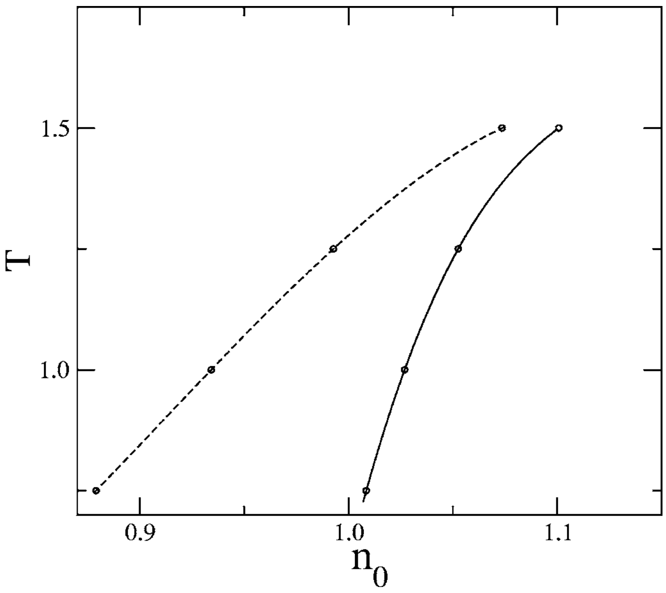

FIG. 9. Coexisting densities of solid phase (solid line) and liquid phase (dashed line) for the Lennard-Jones system at different temperatures T (in units of ϵ/k_B).

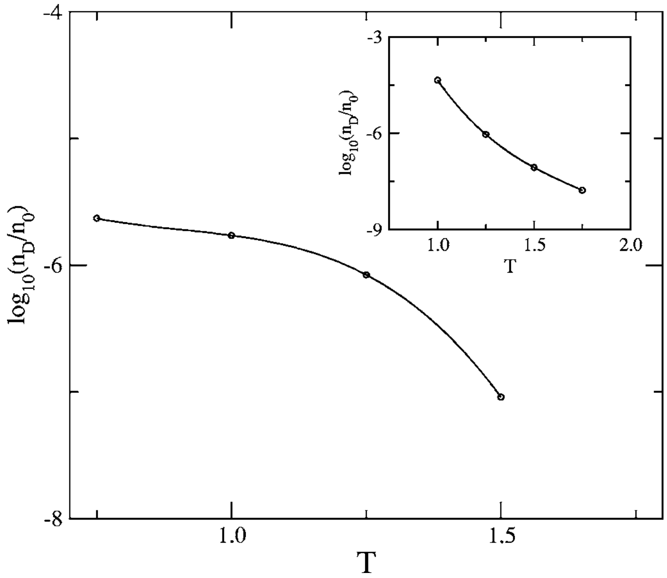

FIG. 10. Relative defect density $\ln(n_D/n_0)$ vs the temperature T (in units of ϵ/k_B) along the solid-liquid coexistence line. The inset shows the corresponding result from Ref. 19

IV. DISCUSSION

We have studied here a simple model for the Lennard-Jones crystal with vacancy defects in the lattice structure. Unlike the hard sphere case, the thermodynamic properties are temperature dependent in this case. Following methods developed for the liquid state, the LJ interaction is divided into a purely repulsive core as well a purely attractive part. We compute the free energy from a DFT approach using a test density function $n(\mathbf{r})$ for the inhomogeneous solid. $n(\mathbf{r})$ is parametrized in terms of Gaussian profiles of WP α. The contribution to the thermodynamic properties of the LJ solid coming from the hard core repulsive part of the interaction potential constitute the so-called reference part. For the purpose of computation, the reference system is identified with a suitable hard sphere system. The total free energy of the imperfect fcc solid is calculated by taking the contribution due to the attractive potential within the mean-field approximation.

The activated behavior displayed in Fig. 4 can be easily justified from a simple model which estimate the optimum free energy cost of creating a vacancy in the solid in terms of an independent parameter[16] ϵ_0 (say). The energy (ϵ_0) represent the energy cost of taking a particle out of the crystal and is to be determined independently. In this model the energy scale is an input and must be evaluated independently from direct simulation[17] or otherwise for an estimation of the defect concentration. In the present work, on the other hand, the activated behavior is obtained without using any such input parameter. The starting point in the present DFT model is the basic interaction potential which acts as an input in the theory in terms of the direct correlation functions $c(r)$. The present work estimates the vacancy concentration in the LJ solid by improving the theoretical model along several lines and calls for a more careful estimation of the vacancy concentration in similar systems with improved experimental and simulation methods.

We obtain the equilibrium defect vacancy in LJ crystal near the freezing decreases in an exponential manner with the inverse temperature at constant density or the pressure. The optimum vacancy density obtained in our model is close to the theoretical result $n_D \sim 7.5\times10^{-5}$ of Ref. 18 in which a different approach to the problem was taken. In that work the two-body Lennard-Jones interaction is considered for the rare gas solid (argon, krypton) and using the Einstein model in the quasiharmonic approximation the Helmholtz free energy with one vacancy is obtained. Our results are also similar to the dependence of the defect density on various thermodynamic parameters seen in this earlier DFT models[19] constructed using the simple Ramakrishnan-Yussouff approach.[20] However in the present work the DFT treatment for the LJ solid is improved along several lines. In Ref. 19 the free energy of the solid state is expressed in a low order perturbative expression around the uniform liquid state. This is a very major approximation for the strongly inhomogeneous solid state. In fact the theory for the perfect crystal was improved (subsequent to the original Ramakrishnan-Yussouff work) with the effective medium approximation using a weighted density functional approximation (WDA)[8] to account for the strong density inhomogeneity in the crystal. In the present work we have applied the modified weighted density functional approximation[13] approach to compute the free energy of the *imperfect solid* with vacancy defects. Furthermore in the earlier work[19] the role of the LJ potential is included only by using the direct correlation $c(r)$ function for the uniform liquid. Here the treatment[7] for the inhomogeneous state of the LJ solid is implemented along the same lines as was done in the theory[1] for the homogeneous LJ liquid case. The two-point distribution function $\tilde{f}_2(r)$ is computed here for the inhomogeneous solid state[7] and is then used in calculating the contribution to the free-energy from the attractive part of the interaction. In earlier works this mean-field contribution is usually ignored or computed by replacing $\tilde{f}_2(r)$ with the liquid state pair correlation function $g(r)$. Although both the works (the present calculation and Ref. 19) are using the same DFT approach the methods of computation involved in each case are therefore quite different. The results in the two cases are comparable near freezing. The detailed comparison is shown in Figs. 7, 8, and 10. Along the coexistence line defect density is found to decrease with the increase of the temperature in both works. The temperature dependence of n_D shows the same activated behavior, with the activation energy being somewhat higher in the present case. It should be noted from Fig. 8 that our model's results are closer to those of the RY model near freezing point and the difference widens as one goes to higher densities which is a trend according to expectation due to the approximations involved in the RY model as pointed out above. The difference between the results from the two models is also listed in Table I.

TABLE I. Comparison of the defect density n_D/n_0 with respect to pressure P (in unit of σ^3/ϵ) for the two different temperatures T (in units of ϵ/k_B). P_m represents the critical pressure at which the free energy of the liquid state becomes higher than that of the crystal making the latter more stable.

T	P_m	P	n_D/n_0 (Present result)	n_D/n_0 (Ref. 19 result)
1.0	2.33	2.10	1.80×10^{-5}	8.01×10^{-5}
		3.00	6.45×10^{-6}	2.26×10^{-6}
		4.17	1.88×10^{-6}	2.00×10^{-8}
1.5	8.82	8.01	5.10×10^{-7}	9.77×10^{-6}
		9.60	1.09×10^{-7}	2.82×10^{-6}
		11.57	8.00×10^{-9}	4.00×10^{-9}

In the present model we have considered the nature of the density profiles for all the sites irrespective of their locations on the lattice to be the same (represented by Gaussian profiles of a single width parameter α). However the strain contribution arising from the distortion of the lattice close to the vacant site play a role in the free energy calculation. At the simplest level such an effect can be included in the present theoretical model of DFT by modifying the test density function.[21] This involves representing the sites immediately adjacent to a vacant site in terms of Gaussian profiles with a different width (from that for the general sites in the bulk away from the vacant site). This extension has not been so far done for the LJ system. Our main focus was to construct the perturbation theory for the Lennard-Jones system and hence for the sake of simplicity we have not extended the model to include a new variational parameter for the distorted sites. We now present the result of extending our model in this direction. We compute here the free energy of the imperfect solid simply in terms of the equivalent hard sphere system having an effective diameter corresponding to the LJ system. The optimum free energy is obtained here by minimizing with respect to the three variational parameters, namely the widths for the normal and distorted sites as well as the defect concentration n_D. We obtain, for example, at $T^*=1.0$ and $n\sigma^3=1.0$, a vacancy concentration of $n_D=7.2\times10^{-6}$ which is of the same order of magnitude as the corresponding result from the simpler model considered above. In Fig. 4, as a comparison with the simplified model we show as an inset the dependence of $\ln(n_d/n_0)$ vs inverse of temperature T^{-1}. It is interesting to note that from the optimized values of the density parameters it follows in a natural way that the width of the distorted sites are usually larger than the normal sites. This conforms to the physical situation that the degree of mass localization is less adjacent to the vacant site. This model can be further refined by including the new density function for the calculation of the mean-field part for the free energy representing the effect of the attractive part of the Lennard-Jones interaction. Another possible way of including the role of distortion near the defects will be relaxing the positions of the lattice points at which the centers of the Gaussian density profiles in the inhomogeneous density function are located. This of course will involve restricting the calculation to a finite size system.

ACKNOWLEDGMENTS

One of the authors (S.P.S.) acknowledges CSIR, India and one of the authors (S.P.D.) acknowledges the IFCPAR Project No. 2604-2 for financial support.

APPENDIX: FREE ENERGY OF THE REFERENCE SYSTEM

The free energy of the hard sphere system of the diameter σ is obtained as a sum of the ideal gas term and interaction or excess free energy term, $F_{\mathrm{HS}}[n(\mathbf{r})]=F_{\mathrm{id}}[n(\mathbf{r})]+F_{\mathrm{ex}}[n(\mathbf{r})]$. The ideal gas part of the free energy is expressed as a sum of two contributions,

$$\beta F_{\mathrm{id}} = \int d\mathbf{r} n(\mathbf{r})\{\ln[\Lambda^3 n(\mathbf{r})] - 1\} + \ln\left(\frac{N!N_D!}{(N+N_D)!}\right), \tag{A1}$$

where Λ is the thermal wavelength. The first term on the right-hand side (RHS) of Eq. (A1) is obtained when the N particles in the system are treated as an ideal gas. The partition function of an ideal gas of N particles involve the phase space integration with a Hamiltonian which is strictly Gaussian in the momentum variables and no spatial dependence. This term is a simple generalization of the ideal gas part of the free energy for the nonuniform density, i.e., $n \to n(x)$. The second term in (A1) represents the configurational free energy (entropic contribution) due to the random location of the N_D vacancies among the N_{PC} lattice sites. The different configurations for the various arrangement vacancies on the lattice are considered to be equivalent. Using the Sterling approximation this term can be expressed in terms of the fraction $\mathcal{A}$ as $N_{PC}[\mathcal{A}\ln\mathcal{A}+(1-\mathcal{A})\ln(1-\mathcal{A})]$. In the limit, strongly localized density profiles in the crystalline state density can be further simplified and approximated in terms of a gaussian centered around a single site. This reduced the ideal gas part of the free energy given in Eq. (A1) to

$$\beta f_{\mathrm{id}}(n) = \left[\frac{3}{2}\ln\left(\frac{\alpha}{\pi}\right) - \frac{5}{2}\right] + \frac{n_{pc}}{n_0}[\mathcal{A}\ln\mathcal{A} + (1-\mathcal{A})\ln(1-\mathcal{A})], \tag{A2}$$

where f_{id} is the ideal gas free energy per particle.

For the excess part of the free energy special techniques has been developed to describe the strongly inhomogeneous crystalline solid. The nonuniform system is represented by an effective liquid having a local density which is a weighted average of the crystal density. Here a suitable weight function is to be chosen for the proper averaging. We use here the modified weighted density approximation[13] in which the excess free energy depends upon the global average $\hat{n}$ of the density rather than the local average density. Thus $F_{\mathrm{ex}} = N f_{\mathrm{ex}}(\hat{n})$, where $f_{\mathrm{ex}}(\hat{n})$ represent the excess free energy per particle of the homogeneous system as a function of the global average density $\hat{n}$. The weighted density $\hat{n}$ is obtained from the self-consistent solution of the integral equation for the equivalent liquid,[13]

$$2f'_{\mathrm{ex}}(\hat{n})\hat{n} = -N^{-1}\int d\mathbf{r}_1 \int d\mathbf{r}_2 c(|\mathbf{r}_1-\mathbf{r}_2|;\hat{n})n(\mathbf{r}_1)n(\mathbf{r}_2) - n_0\hat{n}f''_{\mathrm{ex}}(\hat{n}), \tag{A3}$$

where the prime on the f_{ex} denotes the derivative with respect to density. Equation (A3) is obtained by requiring that the second functional derivative of the MWDA excess free energy yields the correct direct correlation function $c(r)$ in the uniform density limit $n(\mathbf{r}) \to n_0$.[13]

In order to solve $\hat{n}$ for a hard sphere system of diameter σ, we substitute in (A3) the Percus Yevick (PY) solution of direct correlation function $c(r)$ and the corresponding (interaction) free energy f_{ex}, expressed as a function of the packing fraction $\hat{\eta}=\pi\hat{n}\sigma^3/6$,

$$f_{\mathrm{ex}}(\hat{\eta}) = \frac{3}{2}\left(\frac{1}{(1-\hat{\eta})^2} - 1\right) - \ln(1-\hat{\eta}). \tag{A4}$$

The nontrivial task in solving Eq. (A3) is the evaluation of the integral $\mathcal{I}$ (say) in the first term on the RHS, involving products of the densities $n(\mathbf{r})$ at two different points. Using the definition (1) for the density function, $\mathcal{I}$ is obtained in terms of overlapping integrals $A(\mathbf{R})$ of Gaussian profiles centered at two lattice sites separated by a distance $\mathbf{R}$,

$$\mathcal{I} \equiv \sum_{\mathbf{R}} A(\mathbf{R}) = \left(\frac{\alpha}{\pi}\right)^3 \int d\mathbf{r}_1 e^{-\alpha r_1^2} \int d\mathbf{r}_2 c(r_{12}) \sum_{\mathbf{R}} e^{-\alpha|\mathbf{r}_2-\mathbf{R}|^2}. \tag{A5}$$

In Eq. (A5) we have used the notation $r_{12}=|\mathbf{r}_1-\mathbf{r}_2|$ and the summation over R is implied for all pairs of occupied lattice sites. This sum is conveniently evaluated in terms of occupation numbers of lattice points in concentric shells around a given lattice site as center. The occupation numbers Δ_i, for $i=1,2,\ldots$ of different shells are required as an input in this

TABLE II. In the fcc lattice, numbers of occupied sites and the vacant sites in different concentric shells centered around a site lying at a distance R_0 from the vacancy. R_0 is expressed in units of the lattice constant a.

	Number of occupied sites in shell (i)				Number of vacant sites in shell (i)		
R_0	I	II	III	IV	I	II	III
$1/\sqrt{2}$	11	6	24	12	1	0	0
1	12	5	24	12	0	1	0
$\sqrt{3/2}$	12	6	23	12	0	0	1
$\geqslant 2$	12	6	24	12	0	0	0

calculation. For a perfect lattice the set of Δ_i's with any site as origin are identical. However for the imperfect solid the environment of lattice sites close to the vacancy are different. Since the vacancy concentration is very low and the Gaussian profiles are very sharp for the crystalline state, we only count the sites lying within next nearest neighbor distance from the vacancy as special, i.e., having different set of Δ_i's from those in the bulk. The occupation numbers are provided in Table II for the fcc structure. The horizontal rows in Table II, correspond to different values of R_0 which is the distance of the origin from the vacant site. The last row in this table is the case in which the origin is in the bulk, i.e., away from any vacancy by a distance long enough so that overlap of the Gaussian profiles is negligible. The weighted density $\hat{n}$ of the equivalent liquid as a function of the n_D and α is obtained by solving the self-consistent equation (A3). The free energy of the solid is obtained from the PY expression (A4) for the free energy at density $\hat{n}$.

---

*Electronic address: shankar@mail.jnu.ac.in

[1] H. C. Andersen, J. D. Weeks, and D. Chandler, J. Chem. Phys. **54**, 5237 (1971).
[2] J. A. Barker and D. Henderson, J. Chem. Phys. **52**, 2315 (1970).
[3] A. D. J. Haymet, Science **236**, 1076 (1987).
[4] Y. Singh, Phys. Rep. **207**, 351 (1991).
[5] N. W. Ashcroft, Aust. J. Phys. **49**, 3 (1996).
[6] A. de Kuijper, W. L. Vos, J.-L. Barrat, J.-P. Hansen, and J. A. Schouten, J. Chem. Phys. **93**, 5187 (1990).
[7] C. Rascón, L. Mederos, and G. Navascués, Phys. Rev. E **54**, 1261 (1996).
[8] P. Tarazona, Mol. Phys. **52**, 871 (1984).
[9] C. Rascón, L. Mederos, and G. Navascués, Phys. Rev. Lett. **77**, 2249 (1996).
[10] W. A. Curtin and N. W. Ashcroft, Phys. Rev. Lett. **57**, 1192 (1986).
[11] J. K. Percus and G. J. Yevick, Phys. Rev. **136**, B290 (1964).
[12] G. L. Jones and U. Mohanty, Mol. Phys. **54**, 1241 (1985).
[13] A. R. Denton and N. W. Ashcroft, Phys. Rev. A **39**, 4701 (1989).
[14] Martin A. Van der Hoef, J. Chem. Phys. **113**, 8142 (2000).
[15] J. J. Nicolas, K. E. Gubbins, W. B. Streett, and D. J. Tildesley, Mol. Phys. **37**, 1429 (1979).
[16] N. W. Ashcroft and D. Mermin, *Solid State Physics* (Holt, Rinehart and Winston, New York, 1976).
[17] D. R. Squire and W. G. Hoover, J. Chem. Phys. **50**, 701 (1969).
[18] H. R. Glyde and J. A. Venables, J. Phys. Chem. Solids **29**, 1093 (1968).
[19] R. McRae, J. McCoy, and A. D. J. Haymet, J. Chem. Phys. **93**, 4281 (1990).
[20] T. V. Ramakrishnan and M. Yussouff, Phys. Rev. B **19**, 2775 (1979).
[21] Sunil P. Singh, Charanbir Kaur, and Shankar P. Das, Phys. Rev. E **72**, 021603 (2005).